**Atmospheric
Chemistry
and Physics
Discussions**

Diagnostics of the Tropical Tropopause Layer from in-situ observations and CCM data

E. Palazzi[1], F. Fierli[1], F. Cairo[1], C. Cagnazzo[2], G. Di Donfrancesco[3],
E. Manzini[2,4], F. Ravegnani[1], C. Schiller[5], F. D'Amato[6], and C. M. Volk[7,*]

[1]ISAC-Institute for Atmospheric Sciences and Climate, National Research Council, Italy
[2]CMCC-Centro Euro-Mediterraneo per i Cambiamenti Climatici, Italy
[3]ENEA-Ente Nuove Tecnologie Energia e Ambiente, Rome, Italy
[4]INGV-Istituto Nazionale di Geofisica e Vulcanologia, Italy
[5]FZJ, Forschungzentrum Julich, GMBH, Germany
[6]INOA-CNR, Istituto Nazionale di Ottica Applicata, Italy
[7]J.W. Goethe University, Frankfurt, Germany
[*]now at: Department of Physics, University of Wuppertal, Germany

ACPD

9, 11659–11698, 2009

Diagnostics of the TTL

E. Palazzi et al.

Title Page

Abstract	Introduction
Conclusions	References
Tables	Figures

|◄ | ►|
| ◄ | ► |

Back | Close

Full Screen / Esc

Printer-friendly Version

Interactive Discussion

Diagnostics of the TTL

E. Palazzi et al.

Abstract

A suite of diagnostics is applied to in-situ aircraft measurements and one Chemistry-Climate Model (CCM) data to characterize the vertical structure of the Tropical Tropopause Layer (TTL). The diagnostics are based on the vertical tracers profiles, relative vertical tracers gradients, and tracer-tracer relationships in the tropical Upper Troposphere/Lower Stratosphere (UT/LS), using tropopause coordinates.

Observations come from the four tropical campaigns performed from 1998 to 2006 with the research aircraft Geophysica and have been directly compared to the output of the ECHAM5/MESSy CCM. The model vertical resolution in the TTL allows for appropriate comparison with high-resolution aircraft observations and the diagnostics used highlight common TTL features between the model and the observational data.

The analysis of the vertical profiles of water vapour, ozone, and nitrous oxide, in both the observations and the model, shows that concentration mixing ratios exhibit a strong gradient change across the tropical tropopause, due to the role of this latter as a transport barrier and that transition between the tropospheric and stratospheric regimes occurs within a finite layer. The use of relative vertical ozone gradients, in addition to the vertical profiles, helps to highlight the region where this transition occurs and allows to give an estimate of its thickness. The analysis of the CO-O_3 and H_2O-O_3 scatter plots and of the Probability Distribution Function (PDF) of the H_2O-O_3 pair completes this picture as it allows to better distinguish tropospheric and stratospheric regimes that can be identified, first, by their differing chemical composition.

The joint analysis and comparison of observed and modelled data allows us to evaluate the capability of the model in reproducing the observed vertical structure of the TTL and its variability, and also to assess whether observations from particular regions on a monthly timescale can be representative of the fine scale mean structure of the Tropical Tropopause Layer.

1 Introduction

The extreme dryness of the stratosphere was used by Brewer (1949) to deduce that air entered the stratosphere primarily in the tropics, within the so called Tropical Tropopause Layer (TTL) (Fueglistaler et al., 2005). This transition layer has properties both of the troposphere and the stratosphere and, in the tropics, may extend over several kilometers vertically encompassing the tropopause. The TTL is of interest not only because of being the interface between two very different dynamical regimes but also because it acts as a gate to the stratosphere for atmospheric tracers such as water vapour and other short lived substances, which both play an important role for stratospheric chemistry and climate (Holton et al., 1995).

The ascending branch of the Brewer-Dobson circulation transports the mass upward in the tropics from the upper troposphere driving the vertical stratospheric motion. The stratospheric Brewer-Dobson circulation is also key to the "atmospheric tape recorder" signals in water vapour and other compounds like CO_2 (Andrews et al., 1999; Park et al., 2007) and CO (Schoeberl et al., 2006). The tape recorder is the name given to the slow upward movement of trace gases into the tropical stratosphere and apparently all that is required for a tape recorder is a trace gas that varies in concentration with time near the tropical tropopause. The tape recorder in water vapour, in particular, was validated by Mote et al. (1996) using measurements from the satellite-borne Microwave Limb Sounder (MLS) and Halogen Occultation Experiment (HALOE) instruments, showing that air transported upward retains a memory for tropical tropopause conditions for at least 18 months, as it is advected upward by the large scale circulation. The seasonal variation of water vapour in the tropical lower stratosphere, in fact, is clearly tied to seasonality in tropical tropopause temperatures, which are correlated with the seasonal variability of "freeze-drying" process in the upper troposphere and tropical tropopause region (Randel et al., 2001). Freeze-drying mechanism is responsible for the low water vapour values in the lower stratosphere, since air passing through the tropical tropopause has its water vapour mixing ratio reduced to the ice

saturation value at or near the tropopause.

The processes that contribute to the unique properties of the TTL, identified as the zone where the properties of both troposphere and stratosphere can be observed, are subject of long debates and studies, focusing on the use of both observational and model data (Fueglistaler et al., 2009). In-situ observations in the Upper Troposphere/Lower Stratosphere (UT/LS) are unique in terms of accuracy, sensitivity, and resolution but they are sparse for season and regions. Satellite observations, on the other hand, guarantee an extensive geographical coverage and measurement continuity, and can provide a global picture of the lower and middle stratosphere, but their typical resolution cannot describe the required detailed vertical structure of the TTL.

These sets of observations have been intensively used to study the TTL processes and can be exploited also to correctly estimate the capability of current Chemical Circulation Models (CCMs) to reproduce the structure of the TTL. In a recent study, for example, Gettelman and Birner (2007) have discussed the capability of two CCMs in describing the key structural features of the TTL including the mean state and the variability of temperature, ozone, clouds, and thermal structure. They concluded that the TTL features must be largely regulated by the large scale processes, since the TTL structure seemed not altered by sub-grid scale processes such as convection.

The validation of CCMs with observational data sets from in-situ or remote sensing measurements can be improved using diagnostics that are able to reveal peculiar features in the tropical UT/LS tracers distribution. These diagnostics are key indicators of whether the contributions of dynamics and chemistry to the tropical tropopause region are correctly represented in the models, and have been used by several authors to perform comparisons between models and measurements, e.g. in the extratropics. For instance, Pan et al. (2007) showed that the tracers distribution and mixing across the extratropical UT/LS is highlighted when moving from geometric altitude coordinates into tropopause-referenced coordinates or in tracer-tracer space.

In this paper, we perform a joint analysis of the in-situ high-resolution measurements performed on-board the research aircraft Geophysica during the four tropical cam-

Diagnostics of the TTL

E. Palazzi et al.

paigns – APE-THESEO (February–March 1999, Seychelles), TROCCINOX (January–February 2005, Brazil), SCOUT-Darwin (November–December 2005, Australia), and SCOUT-AMMA (August 2006, West-Africa), and the ECHAM5/MESSy CCM. A set of diagnostics, which have been successfully applied in the extratropical tropopause region (Pan et al., 2007; Hegglin et al., 2009), are here applied to observational and model data in the Tropical Tropopause Layer, to highlight some features of the TTL vertical structure and its regional/temporal variability. The diagnostics are based on the analysis of the vertical profiles of water vapour, ozone, and nitrous oxide and of the relative vertical ozone gradients, in a tropopause-referenced coordinate, and on $CO-O_3$ and H_2O-O_3 correlations.

The aircraft measurements performed during the tropical campaigns include observation of a wide number of chemical species in the whole TTL height, in peculiar regions and seasons. So, these observations are actually used to characterize the TTL vertical variability of different species like water vapour, O_3, N_2O, and CO. This analysis is applied on a straightforward way to the model data, encouraging in this way a comparison between the model and the observations. The comparison between the ECHAM5/MESSy CCM and the in-situ dataset aims at estimating how the vertical structure of the tropical transition layer and its variability can be inferred from the joint analysis of observed and modelled data through the application of the specific aforementioned diagnostics. Moreover, the comparison aims at evaluating how the simulations reproduce the observed vertical structure of the TTL and assessing to which extent observations from different time periods and locations can be considered as representative of the whole TTL fine scale mean structure.

The paper will be arranged as follows. Section 2 presents the observations and the main characteristics of the model run. Section 3 describes the methodology used to compare the observations and the ECHAM5/MESSy data. The diagnostics used, such as tropopause coordinates, tracer-tracer correlations, and relative vertical tracer gradients are described. Section 4 provides a direct comparison of the measured and modelled vertical tracers profiles and the relative vertical ozone gradient around

the tropical tropopause. In Sect. 5, we focus on the analysis of CO-O_3 and H_2O-O_3 correlations in the TTL, for both the model and the observations. Section 6 gives the main conclusions of this work.

2 Description of the campaigns and the model data

2.1 The measurement campaigns

The experimental data presented in this paper were obtained during four tropical measurement campaigns performed at different times and locations with the high-altitude M55 Geophysica aircraft. APE-THESEO (Airborne Platform for Earth observation – contribution to the Third European Stratospheric Experiment on Ozone) was performed from 15 February to 15 March, 1999, in the Seychelles (Stefanutti et al., 2004). TROC-CINOX (TROpical Convection, Cirrus and Nitrogen Oxides Experiment) was carried out in January and February 2005 in Brazil (ACP special issue "TROCCINOX-Tropical convection and its impact on the troposphere and lower stratosphere"). SCOUT-Darwin (Stratospheric-Climate Links with Emphasis on the Upper Troposphere and Lower Stratosphere) took place in Australia, in November–December 2005 (Vaughan et al., 2008). SCOUT-AMMA (African Monsoon Multidisciplinary Analyses) was performed in August 2006 in Burkina Faso, West Africa (Law et al., 2009). The red boxes in Fig. 1 indicate the regions where the aircraft flights planned in the frame of the four campaigns took place (the measurements taken during the transfer flights have not been included in our analysis).

The scientific objectives of the campaigns were to study chemical processes and transport into the TTL and across the tropopause. In particular, all the campaigns focused on the analysis of such processes in deep convective systems, such as the continental convection over Brazil during TROCCINOX (Chaboureau et al., 2006), the isolated "Hector" storms over the Northern Australian archipelago during SCOUT-Darwin (Brunner et al., 2009) and the African monsoon during SCOUT-AMMA. Con-

[ACPD](#)

9, 11659–11698, 2009

Diagnostics of the TTL

E. Palazzi et al.

Title Page

Abstract	Introduction
Conclusions	References
Tables	Figures

◄ | ►

◄ | ►

Back | Close

Full Screen / Esc

Printer-friendly Version

Interactive Discussion

sequently, all the campaigns included a fraction of flights useful to study the impact of convection on the mean chemical structure of the upper troposphere. Therefore, a bias toward convectively influenced observations can be expected, markedly in the SCOUT-Darwin campaign and to a lesser extent in the SCOUT-AMMA and TROCCI-NOX campaigns. Direct convection events can for example alter the water budget at the tropical tropopause, leading to a moistening of the lower stratosphere at least locally (Chaboureau et al., 2006; Corti et al., 2008). APE-THESEO measurements, which took place during a relatively quiescent period, can be considered the less-convectively influenced dataset. In our analysis, no filters have been applied on the observations to remove the impact of the small-scale transport processes related to convective activity.

Table 1 lists the instruments used on board the aircraft Geophysica for the measurement of the atmospheric compounds considered in our study.

2.2 Numerical model

The atmospheric chemistry general circulation model used in our study consists of ECHAM5 (Roeckner et al., 2003, 2006) coupled with the Modular Earth Submodel System, MESSy. This model includes a comprehensive representation of clouds, radiation, multiphase chemistry and emission-deposition processes (Jöckel et al., 2006). The model computes the atmospheric dynamics up to wavenumber 42 using a triangular truncation (T42), which allows to predict the prognostic variables every 15 min. The associated quadratic Gaussian grid, where physical and chemical parameterizations are calculated, is of approximately 2.8° in latitude and longitude (Roeckner et al., 2006). The vertical grid resolves the atmosphere with 90 vertical layers reaching up to 0.01 hPa (~80 km altitude). The mean layer thickness in the lower and middle stratosphere is about 700 m, which allows for a resolution high enough to internally generate the quasi-biennial oscillation (QBO), as shown by Giorgetta et al. (2006). The vertical resolution in the tropopause region is higher, about 500 m (6–10 hPa).

Further general description of the model setup can be found in Jöckel et al. (2006); the radiation scheme is accurately described in Cagnazzo et al. (2007) and information

about coupling of ECHAM5 with MESSy can be found in Jöckel et al. (2005) (see also http://www.messy-interface.org/).

The cloud microphysics scheme implemented in the CCM is described in Lohmann and Roeckner (1996) and includes phase changes between the water components (condensation/evaporation, deposition/sublimation, and freezing/melting) and precipitation processes (autoconversion, accretion, and aggregation). Moreover, the evaporation of rain and the melting of snow are considered as well as the sedimentation of cloud ice.

The simulation presented here is a three year run, forced with climatological sea surface temperatures (SSTs), so the effect of El Niño or La Niña are not included. The model is not forced through nudging on dynamical variables towards atmospheric analyses and hence it performs a free run both in the troposphere and in the stratosphere.

For the representation of natural and anthropogenic emissions and the boundary conditions for the chemical species considered in this study, we refer to the detailed description by Kerkweg et al. (2006). We have used 3-D fields of the chemical and dynamical variables taken at 12:00 UTC every day, in the height range between 300 hPa and 10 hPa.

Figure 2 shows the variation of the model monthly mean temperature (top) and water vapour (bottom), averaged between 15° S and 15° N. The monthly means are divided by the time mean value at each level. The isentropic surface at $\theta = 380$ K (here used as a proxy of the tropical tropopause), the zonal mean zonal wind at 40 hPa, and the temporal location of the four measurement campaigns (SC=SCOUT-Darwin, TH=APE-THESEO, AM=SCOUT-AMMA, TR=TROCCINOX) considered in this study are also shown.

Figure 2 clearly shows the presence of a tape recorder signal in the ECHAM5/MESSy water vapour. H_2O follows an annual cycle between about 150 and 100 hPa that propagates upward in the whole domain under analysis. Minima of H_2O at the tropopause are found in the NH winter (corresponding to APE-THESEO, TROCCI-NOX, SCOUT-Darwin temporal and spatial domains) while the maxima occur in the NH

ACPD

9, 11659–11698, 2009

Diagnostics of the TTL

E. Palazzi et al.

Title Page

Abstract	Introduction
Conclusions	References
Tables	Figures

| ◄ | ► |
| ◄ | ► |

| Back | Close |

Full Screen / Esc

Printer-friendly Version

Interactive Discussion

summer (SCOUT-AMMA), when the temperatures at the tropopause are lowest and highest, respectively. In Sect. 4.2 it will be shown that this seasonal variability in water vapour is seen in the observational data as well, and agrees with the one reproduced by the model. Nevertheless, the temperature profiles measured during the four aircraft campaigns will not be discussed in this paper.

The simulated H_2O tape recorder can be compared to the MLS water vapour shown in the paper by Liu et al. (2007) (Fig. 1a). At 100 hPa the greater (lower) than one water vapour values roughly span from June to November (November to June) for both MLS and ECHAM5/MESSy. At 70 hPa the agreement between MLS and the model is still consistent, with a one-month phase shift. At 50 hPa, on the other hand, the MLS water vapour greater (lower) than one values span from September to May (May to September), while for ECHAM5/MESSy from September to March (March to September). The comparison between the MLS and ECHAM5/MESSy water vapour tape recorder gives an overall good agreement in the lowermost stratosphere (pressure <70 hPa), while a phase shift of approximately two months appears at 50 hPa.

The ECHAM5/MESSy water vapour tape recorder is also in agreement with the results obtained by Lelieveld et al. (2007), who compared the ECHAM5/MESSy1 model with realistic tropospheric nudging for the period 1996–2005 to the HALOE water vapour observations.

3   Methodology

The exchange of chemical constituents between the upper troposphere and the lower stratosphere takes place across the tropopause, which is often marked by an abrupt transition in the values of atmospheric concentration of compounds such as water vapour, ozone, and various nitrogen oxides. However, observations of temperature, winds, and atmospheric trace gases suggest that the transition from troposphere to stratosphere occurs in a layer, rather than at a sharp tropopause. In the tropics this layer is known as the Tropical Tropopause Layer (Fueglistaler et al., 2009). The TTL

can be qualitatively defined as the region where the tropospheric convection effect remains but no longer dominates the setting of the temperature structure which – as in the stratosphere – is mainly affected by radiative processes (Thuburn and Craig, 2002). However, the TTL is currently not well or consistently defined, leading to various definitions of its vertical boundaries and thickness (Gettelman and Forster, 2002; Highwood and Hoskins, 1998; Sherwood and Dessler, 2001; Folkins et al., 1999; Vömel et al., 2002).

In this study, a tropopause coordinate (i.e., using vertical profiles of a variable of interest relative to the tropopause height or pressure) is used rather than the geometric altitude or pressure as the vertical coordinate, since it highlights the characteristics of tracers transition across the tropopause and the climatological features of the chemical distribution in the UT/LS, minimizing the effects of geophysical and meteorological variability (Pan et al., 2007). The tropopause-referenced vertical profiles of chemical tracers are indeed more compact than if they were plotted in geometric altitude/pressure or potential temperature coordinates, and reveal the sharp gradient change between tropospheric and stratospheric mixing ratios (Pan et al., 2004; Hoor et al., 2004; Hegglin et al., 2006, and references therein).

In addition, the tropopause coordinate system facilitates the identification and representation in Chemistry-Climate Models of the specific structure of a given tracer across the tropopause and within the TTL, allowing for a direct comparison between model data and measurements and for process-oriented validations of CCMs.

By convection of the World Meteorological Organization (WMO), the tropopause is defined as the lowest level at which the temperature lapse rate becomes less than $2\,K\,km^{-1}$, provided that the average lapse rate between this level and all higher levels within 2 km does not exceed $2\,K\,km^{-1}$ (WMO, 1957). This conventional thermal definition of the tropopause has been used throughout the present paper. Nevertheless, it is known that the tropical tropopause corresponds roughly to the isentropic surface $\theta \approx 380\,K$ (in the annual mean), a definition that enhances the quasi-material behaviour of the tropopause. The use of $\theta = 380\,K$ as a proxy for the tropical tropopause as been

done in Sect. 2.2, Fig. 2.

Following the recent work by Hegglin et al. (2009), a relatively new approach is used here for the representation of the vertical structure of the TTL based on chemical tracers: the use of relative vertical tracer gradients (the ratio between the vertical tracer gradients and the tracer concentrations), plotted in tropopause coordinates, which are equivalent to the vertical gradients of the logarithm of the tracers concentration (Randel et al., 2007). This formulation is particularly useful to identify the vertical distribution of the layers where tracers characterized by strong gradients across the tropopause show high variability and allows to give a measure of the TTL thickness. The analysis of the tracers relative vertical gradients can be applied also to model-measurement comparisons to test the capability of CCMs to capture the ensemble of dynamical and chemical processes that determine the transition in tracer distributions across the tropopause transition region.

To characterize the chemical transition across the tropopause, use can also be done of the theory of relationships between a tropospheric and a stratospheric tracer. Until now, this approach has been widely applied in the extra-tropics (Pan et al., 2007; Hegglin et al., 2009) to derive the extratropical tropopause layer depth using CO-O_3 and H_2O-O_3 correlations. In an atmosphere with ideally no mixing between troposphere and stratosphere (i.e., where the tropopause would act as a perfectly impermeable barrier to vertical transport) the correlation between a tropospheric and a stratospheric tracer would have the typical *"L"* shape predicted from the theory (Plumb, 2007), with a nearly linear relationship between the tracer mixing ratios for both the tropospheric and stratospheric branches. This shape is likely expected in the tropics, at least for the H_2O-O_3 pair, since cross-tropopause mixing is small and upward motion from the troposphere to the stratosphere is associated with dehydration at the tropopause (Brewer, 1949). Nevertheless, Pan et al. (2007) showed that, in the extra-tropics, the correlations between the stratospheric O_3 and the tropospheric CO or H_2O move from the linearity an exhibit a curvature, which is associated to the importance of mixing and stratosphere-troposphere exchange mechanisms that lead to the erosion of the

Title Page

Abstract	Introduction
Conclusions	References
Tables	Figures

| ◄◄ | ►► |
| ◄ | ► |

| Back | Close |

Full Screen / Esc

Printer-friendly Version

Interactive Discussion

sharp transition between tropospheric and stratospheric regimes. This diagnostic facilitates the understanding of a finite chemical transition layer that encompasses the tropopause, with partly tropospheric, partly stratospheric character and allows to derive the transition region depth (Hegglin et al., 2009).

5   In this paper, the theory of the correlation between a tropospheric and a stratospheric tracer is applied to the TTL, and used to identify the chemical transition across the tropical tropopause, using both the H_2O-O_3 and CO-O_3 relationships. Since the structure found in the form of tracer-tracer scatterplots can strongly reflect sampling (Hegglin and Shepherd, 2007), the use of joint probability density functions (PDFs) is in some
10 circumstances preferable: an example of such an approach is shown for the H_2O-O_3 correlation.

    Table 2 specifies the latitudinal and longitudinal domain and the temporal collocation of each measurement campaign analyzed in this study, and indicates the number of model grid points within each box. The phase of the QBO at 40 hPa relative to each
15 campaign time period is also reported.

    For the observations, the chemicals concentrations measured during the Geophysica flights (one flight per day) have been averaged within the geographical box (see also Fig. 1) and through the duration (about one month) of each campaign, in order to obtain a unique profile representative of the observations for a selected region, month, and
20 QBO phase.

    For the model as well, one unique averaged vertical profile for each species has been considered for each of the three model years. However, in this paper, we have not focused on the model interannual variability and the observed mean vertical profile of each species has been compared to the modelled one using the criterion of matching
25 the observed QBO phase with the QBO internally generated by the model.

4 Measured versus modelled vertical profiles

In this section, we analyze the mean vertical behaviour of ozone (Fig. 3a and 4), water vapour (Fig. 5), and nitrous oxide (Fig. 6) from each campaign observations (black lines) and the model data (red lines). The shaded green area includes the mean vertical tracers profiles (or the relative tracers gradients in Fig. 4) from the three model years, and the black dash-dotted line indicates the thermal tropopause calculated from the observations. The tropopause calculated from the model temperature and pressure values is not shown. Each panel in Figs. 3a, b, 5, and 6 corresponds to the region and time period of each campaign.

4.1 Ozone

Ozone is a tracer frequently used for studies of the TTL and troposphere-stratosphere exchange in general (e.g. Folkins et al., 1999), due to the fact that it is much more abundant in the stratosphere than in the troposphere.

In both the modelled and observed vertical profiles shown in Fig. 3, an upper tropospheric regime, characterized by nearly constant and less than 100 ppbv ozone mixing ratios, a transition zone between about -15 and 15 hPa in which air starts to assume some of the chemical characteristics of the stratosphere, and a lower stratospheric regime where ozone concentrations strongly increase with height due to photochemical production, are observed. Though these three regimes in the ozone vertical behaviour are visible in both the modelled and the observed ozone profiles, some differences occur between them, that are in part related to the specificity of each campaign.

During SCOUT-Darwin (bottom left panel) and SCOUT-AMMA (bottom right panel), for instance, the model profiles are characterized, respectively, by higher ozone mixing ratios then those observed throughout the entire vertical range considered and in the lower stratosphere, while the model-measurements agreement can be considered satisfactory in the case of APE-THESEO and TROCCINOX campaigns.

SCOUT-Darwin took place during the pre-monsoon season, characterized by vigor-

ous convection including the development of a mesoscale system known as "Hector" (Brunner et al., 2009). Therefore, convection occurred during this campaign, and the lower observed ozone mixing ratios (compared to the ones measured during the other campaigns) in the upper troposphere can be interpreted as a consequence of convec-
5   tive detrainment of ozone-poor low-level air. Moreover, since in the tropical boundary layer over the oceans net ozone destruction occurs, local transport patterns with enhanced meridional transport of air from Pacific Equator and the occurrence of deep convection can be invoked together to explain the ozone reduction in the lower stratosphere. We also report in the bottom left panel of Fig. 3, the ozone mixing ratios
10 measured over the Fiji Islands (18.13° S, 178.40° E) in the time period corresponding to the SCOUT-Darwin campaign by the ozonosondes belonging to the SHADOZ network (Thompson and Witte, 1999). It can be noticed that ECHAM5/MESSy agrees well with the SHADOZ data since these latter are much less influenced by local convection and by the "Hector" system that the aircraft measurements.
15   With regard to SCOUT-AMMA, the observational strategy followed during this campaign led to a fraction of observations (about 30%) influenced by local convection, that should explain the low ozone values in the lowermost stratosphere. The analyses carried out so far on the SCOUT-AMMA measurement database have shown that all observations constitute an ensemble adequate and representative of the mean aver-
20 age conditions of the TTL of that region during August 2006 (Law et al., 2009).
        In Fig. 4, the observed and modelled ozone relative vertical gradients, expressed in tropopause coordinates (see Sect. 3) are shown, the color notation being the same as in Fig. 3. The modelled gradients shown in Fig. 4 have the same general vertical structure in the different geographical and temporal domains considered, which is
25 characterized by a minimum located from 10 to 20 hPa above the thermal tropopause that marks the beginning of stratospheric ozone increasing concentrations and a local maximum located from 5 to 10 hPa below the thermal tropopause. In between lies the region that can be actually considered the transition between tropospheric and stratospheric regimes and that is no more than 30 hPa-thick (from 15 to 30 hPa, depending

on the campaign).

The observations generally confirm the picture illustrated by the model, though they are much more scattered due to local effects, especially duing SCOUT-Darwin and TROCCINOX. For APE-THESEO and SCOUT-AMMA, a satisfactory model-measurements agreement is found.

The vertical tracer gradients approach has been used by Hegglin et al. (2009) to supply a measure of the extratropical tropopause transition layer depth using the vertical gradients of CO and O_3 mixing ratios from the limb-viewing Atmospheric Chemistry Experiment-Fourier Transform Spectrometer (ACE-FTS). ACE-FTS has provided accurate measurements of numerous chemical species with high vertical resolution (better than 1 km) in the UT/LS.

4.2 Water vapour

Water vapour is one of the key tracers for troposphere-stratosphere exchange that led Brewer (1949) to conclude that air enters the stratosphere primarily in the tropics (see Sect. 1). In general, tropical water vapour concentration vertical profiles are characterized by large H_2O values in the troposphere, a region with a pronounced tracer gradient with very low concentrations near the tropical tropopause, and smaller values in the lower stratosphere compared to the tropospheric mixing ratios. Very low values of the water vapour mixing ratio, in fact, extend upward from the minimum, which is only a few part per million by volume and far lower than typical tropospheric values, within a few kilometers of the tropical tropopause. The increase of water vapour concentrations above the minimum at tropopause levels can be due to in-mixing of stratospherically older air masses with increased water concentrations (due to oxidized methane), and, to a lesser degree, to in-situ methane oxidation or sporadic overshooting convection.

These distinct features in the TTL water vapour distribution are in the main found in both the modelled and observed water vapour mixing ratio vertical profiles shown in Fig. 5. For each campaign analyzed, the modelled water vapour mixing ratios agree well with the observed ones, both above and below the tropopause. At the tropopause,

the dehydration mechanism can be considered to be well captured by the model, even if a dry bias of about −1.5 ppmv can be identified in the model with respect to the observations in the case of SCOUT-AMMA (bottom right). For the other campaigns, the differences between the modelled and observed H_2O mixing ratios at the tropopause are less significant and, anyhow, they are included in the interannual variability of the three model years (shaded area) and in the standard deviations of the observations. Lelieveld et al. (2007) compared results from the ECHAM5/MESSy1 CCM to satellite HALOE water vapour observations for the period 1996–2005 and, based on a model evaluation between 30° S and 30° N latitude, they found a dry bias in the model of about −0.5 ppmv in the 100 hPa–75 hPa region.

In general, the largest differences between the observed and modelled water vapour vertical profiles arise in the upper troposphere where, as expected, higher H_2O concentrations are observed in convectively influenced regions. See, for instance, the observed H_2O peak at 20 hPa below the tropopause during SCOUT-Darwin. This is also confirmed by the high variability of the measured profiles, and a likely sampling bias of air masses which are influenced by local convection.

As mentioned above, convection can also occasionally enhance water vapour mixing ratios in the lowermost stratosphere. During the SCOUT-Darwin campaign, for instance, overshoot was measured during several flights (Corti et al., 2008), leading to the high H_2O mixing ratios between −40 and −20 hPa shown in Fig. 5.

Figure 5 also shows that the tropopause (dash-dotted line) is dryer during the NH winter (APE-THESEO, SCOUT-Darwin and TROCCINOX campaigns) while it is moister during the NH summer (SCOUT-AMMA). It has been already pointed out in Sect. 1 and shown in Fig. 2, in fact, that a likely implication of the freeze-drying basic mechanism occurring at or near the tropopause and responsible for the low water vapour values in the lowermost stratosphere, is that H_2O mixing ratios of air entering the tropical stratosphere should vary seasonally in phase with the annual cycle of tropical tropopause temperature.

4.3 Nitrous oxide

N_2O is a tracer that has a tropospheric source and a stratospheric sink, which makes it a chemical species of interest for TTL studies. In fact, it is destroyed by $O(^1D)$ only at altitudes well above the tropopause and air with low N_2O values in the upper part of the TTL therefore is expected to have some stratospherically older origin.

The measured and modelled vertical profiles of N_2O in Fig. 6 show, in general, nearly uniform tropospheric concentrations and a decrease from the tropopause level upward. N_2O is observed to have its largest stratospheric mixing ratios immediately above the tropical thermal tropopause, matching tropospheric values. The profiles shown in Fig. 6 moreover suggest that in-mixing of stratospheric air masses with low N_2O concentrations is rare below the tropopause. The tropospheric value for N_2O has increased of about 1 ppb/yr between 1999 and 2006 (updated from Prinn et al., 2000). However, since the model does not include the actual tropospheric growth rates, the observed N_2O mixing ratios in the upper troposphere are generally higher then the simulated ones (not shown). The observed mean profiles have been scaled with a factor for each campaign, such that tropospheric observed values match those of the model.

The best model-measurements agreement is found for APE-THESEO (located in the inner tropics, see Fig. 1) and for SCOUT-AMMA. Because of the location at about the edge of the tropical pipe, the observations during TROCCINOX show a decrease of N_2O at lower altitudes (Konopka et al., 2007). During SCOUT-Darwin, the negative phase of the QBO, denoting occurrence of westerly winds, led to a less intense dynamical barrier in the subtropics (Shuckburgh et al., 2001), leading to increased meridional transport and, again, layers of low N_2O mixing ratios. In the case of TROCCINOX and, despite the sparseness of observations of SCOUT-Darwin, moreover, the N_2O gradient above the tropopause is sharper in the observations than in the model. Moreover, both observations and model data, show a higher variability compared to the other two campaigns, as denoted by the larger standard deviations.

5 Tracer-tracer correlations in the TTL

In this section, the TTL morphology is investigated from the perspective of chemical composition through the use of tracer-tracer correlations. Working in the tracer-tracer space is useful to reveal characteristic tracer features of different air masses due to specific dynamical and transport processes. In the extratropics, this approach has been widely used to derive the transition layer depth in terms of the distance between its top and bottom from the thermal or dynamical tropopause (Pan et al., 2007; Hegglin et al., 2009). However, only few applications to the TTL can be found in literature (e.g., Hegglin et al., 2009).

As mentioned in Sect. 3, the correlations in the tropics are expected to have the classical "*L*" shape, due to the small cross-tropopause mixing and slow ascent of the air parcels.

In particular, the relationships between the pairs CO-O_3 and H_2O-O_3 will be investigated (Figs. 7 and 8, respectively) using the tracer mixing ratios measured during the four tropical Geophysica campaigns and the ones reproduced by ECHAM5/MESSy. The model data include all the point collocated within the four red boxes shown in Fig. 1.

The tracer-tracer correlation points in Figs. 7 and 8 have been colored according to 12 hPa-thick pressure intervals defined a priori. The PDF of the H_2O-O_3 correlation is also shown exemplary for the region and time period of the SCOUT-Darwin campaign (Fig. 9).

5.1 CO vs. O_3

Figure 7 shows the correlation of CO with O_3 for ECHAM5/MESSy (left column) and the observations from only three of the four campaigns considered in this study (TROC-CINOX, SCOUT-Darwin and SCOUT-AMMA, in the right column from the top to the bottom), since CO data were not measured during APE-THESEO.

In general, the CO-O_3 relationships shown in Fig. 7, rather then the "*L*" shape ob-

Diagnostics of the TTL

E. Palazzi et al.

⏮ | ⏭

◀ | ▶

Back | Close

Full Screen / Esc

Printer-friendly Version

Interactive Discussion

served in the extratropical UT/LS, form a smoother curve. This is mainly due to the chemical lifetime of CO, which is comparable to the transport timescales on which troposphere-to-stratosphere transport occurs and makes CO a "pure" transport tracer.

The black solid lines in Fig. 7 represent the empirical stratospheric and tropospheric CO-O_3 relationships, derived using data points with CO<30 ppbv for stratospheric and O_3<70 ppbv for tropospheric. CO decreases from a range of tropospheric concentrations depending on the campaign, towards its stratospheric steady value of around 30 ppbv, reached at about 10–15 hPa above the tropopause.

Overall agreement is found in the case of SCOUT-AMMA between the modelled (bottom left panel) and observed (bottom righ panel) CO-O_3 correlation. The transition region between tropospheric and stratospheric regimes, in fact, is characterized by similar ozone mixing ratios (from ~80 ppbv to ~450 ppbv) and CO mixing ratios (from ~30 ppbv to ~80 ppbv). For TROCCINOX (first row panels) and SCOUT-Darwin campaigns (middle panels), on the contrary, some differences between the model and the observations can be noticed. The transition region for both these campaigns, as deduced from the model data, occurs for a smaller range of O_3 values (from ~90 ppbv to ~350 ppbv) as well as of CO values (from ~30 ppbv to ~60 ppbv) than those emerging from the observations. The structure of the transition region inferred from TROCCINOX observations, for instance, shows the clear impact of in-mixing from mid-latitudes (due to the fact that this campaign was performed close to the subtropics), which alters and shifts the overall CO-O_3 scatter plot: it lies nearly completely outside the empirical no-mixing lines and is characterized by higher values of CO (from ~30 ppbv to >120 ppbv) and typically stratospheric O_3 mixing ratios.

5.2 H_2O vs. O_3

Figure 8 shows the correlation of H_2O with O_3 for ECHAM5/MESSy (left column) and the observations from the four campaigns analyzed (APE-THESEO, TROCCINOX, SCOUT-Darwin and SCOUT-AMMA, in the right column from the top to the bottom).

In spite of inter-campaigns differences, H_2O-O_3 correlations have the theoretical

tropical "*L*" shape, that results from the small cross-tropopause mixing and small ascent of air parcels that experience dehydration at tropopause levels. H_2O is a less pure tracer than CO. Moreover, the transition between the tropospheric and the stratospheric branches occurs at lower H_2O mixing ratios during winter (APE-THESEO, TROCCI-NOX, SCOUT-Darwin campaigns) than during summer (SCOUT-AMMA campaign), reflecting the seasonal cycle in tropopause temperatures (lower temperatures during winter). The transition occurs around the thermal tropopause or slightly below and involves a layer which is no more than 25–30 hPa thick, depending on the specificity of each campaign.

For SCOUT-AMMA (bottom panels in Fig. 8), both model data and the measurements lie on well separated tropospheric and stratospheric branches with a relatively narrow transition zone in between (∼15 hPa thick). From a chemical point of view the transition region includes H_2O mixing ratios from about 2 to 5 ppmv (model) and 3 to 7 ppmv (observations), in agreement with the ECHAM5/MESSy dry bias discussed in Sect. 4.2, and O_3 mixing ratios less then 200 ppbv, in both the model and the observations.

For the other three campaigns, besides the evidence of dehydration mechanism at tropopause levels, which is a common feature in both the modelled and observed H_2O-O_3 scatter plots, situation is more complicated that for SCOUT-AMMA. For SCOUT-Darwin, for instance, the scatter plot shows a noticeable region of mixing (for H_2O mixing ratios >4 ppmv) in the model, and a less extended region of mixing with more coherent hydrated layers around 12 and 24 hPa above the tropopause in the observations.

Figure 9 shows the two-dimensional PDFs of H_2O-O_3 pairs calculated from the model (left) and the observations relative to the SCOUT-Darwin campaign area and time period. Use of probability density functions in this context has demonstrated to be very useful to provide a detailed picture of key aspects of transport across the tropical tropopause (e.g. Sparling, 2000). The data were binned into H_2O and O_3 bins with widths of 0.1 ppmv and 25 ppbv, respectively, and normalized with respect to the total

number of measurements used in the evaluation. Three well separated regimes are visible in both the observed and modelled H_2O-O_3 PDFs. The tropospheric regime is characterized by a nearly constant O_3 value and variable H_2O mixing ratios, while the stratospheric regime is characterized by a nearly constant H_2O value and variable O_3 mixing ratios. In between, a region where the probability to have chemical character-istics of both the troposphere and the stratosphere is higher than in the two branches, separately. This is particularly well visible in the plot obtained from the measurements.

Maxima in the joint PDFs indicate the regions where mixing is favoured and irre-versible homogenization likely occurs, similar to maxima found in 1-D PDFs of strato-spheric tracers, which indicate the presence of the well mixed regions; minima in the joint PDFs occur likely in the two separated branches, indicating that mixing in these re-gions is limited, similar to the minima found in 1-D PDFs of stratospheric tracers, which indicate the presence of mixing barriers (Sparling, 2000; Neu et al., 2003; Hegglin and Shepherd, 2007).

The example shown in Fig. 9 supports the fact that the PDF approach is helpful to as-sess the statistical relevance of the observational sampling; for instance, the hydrated layers above the tropopause visible in the observations during the SCOUT-Darwin cam-paign (Fig. 8, third row on the right) are not visible in the joint PDF shown in the top panel of Fig. 9. This implies that the fraction of measurements influenced by convection in the lower stratosphere are negligible and do not impact on the statistical properties of the H_2O-O_3 correlation.

6 Conclusions

The TTL is a region of interest because of being the interface between the very dif-ferent dynamical and chemical tropospheric and stratospheric regimes and because it determines the entry of atmospheric tracers such as water vapour and the short-lived substances in the stratosphere.

A decade of observational activity in the tropical UT/LS with high resolution in-situ in-

struments on board stratospheric research aircrafts has built up a considerable dataset that allows to partially overcome the drawback due to the spatial and temporal sparseness of such kind of data, making use of appropriate diagnostics that capture the key aspects of TTL transport and interrelationships between different species.

A good representation of the TTL in Chemistry Climate Models is a challenge, due to the difficulty of understand and correctly simulate the TTL radiative, chemical and dynamical processes and their connections. The vertical resolution of CCMs is often not adequate to capture the small-scale variability of the tracer fields and processes in this relatively thin layer, and the horizontal resolution can also be a limit, since convection that transport compounds from the emission sources to the upper troposphere is parameterized.

In this paper, a suite of specific diagnostics have been applied to the in-situ high-resolution measurements performed on board the aircraft Geophysica during the four tropical campaigns (APE-THESEO, TROCCINOX, SCOUT-Darwin, SCOUT-AMMA) and to the ECHAM5/MESSy CCM data. These diagnostics consist of the vertical mixing ratio profiles and relative gradients of selected compounds (ozone, water vapour, and nitrous oxide), an on tracer-tracer correlations (CO-O_3, H_2O-O_3), all expressed in tropopause coordinates. They corroborate the existence of a tropical tropopause transition region and allow to characterize it in terms of chemical vertical distribution, thickness, and variability. They moreover facilitate comparisons of observational and model data (Pan et al., 2007) and provide a suite of tools for testing the ability of CCMs to simulate the TTL structure.

The analysis of the O_3, H_2O, and N_2O vertical profiles and the ozone relative vertical gradient in tropopause coordinates has revealed, in fact, the existence of a finite tropical transition layer about the tropopause (the TTL) having characteristics of both the troposphere and the stratosphere. The transition between the two regimes occurs within this layer where the aforementioned species exhibit their greatest gradient changes (see Figs. 3, 4, 5, 6). The TTL encompasses the thermal tropopause that acts as a barrier to vertical mixing. The ozone relative vertical gradient, in particular,

Printer-friendly Version

Interactive Discussion

has allowed to deduce that the transition between the tropospheric and stratospheric regimes occurs within a region that extends from where the gradient exhibits a local maximum (from about 5 hPa to 10 hPa below the tropopause) to where the gradients exhibits a minimum and ozone concentrations start to increase (from about 10 hPa to 20 hPa above the tropopause) towards their stratospheric values.

The existence of a region where the tropospheric and stratospheric regimes in chemicals distribution co-exist is enhanced using the correlation between a tropospheric (typically CO or H_2O) and a stratospheric (typically O_3) tracer. In the tropics, a classical L shape is found in the H_2O-O_3 correlation, where vertical transport across the tropopause in mainly upward into the overworld and the low temperatures at the tropopause determine the dehydration of air entering the stratosphere. On the other hand, the CO-O_3 correlation has a smoother shape than the H_2O-O_3 relationship , because CO is a purer tracer for transport than H_2O in this region (the chemical lifetime of CO is comparable to the transport timescales characterizing troposphere-to-stratosphere transport).

Depending on the location in the tropics and on the season, the TTL derived from H_2O-O_3 extends roughly from –20 to 20 hPa (P-TP coordinate), being thinner in summer than in winter. The TTL derived from CO-O_3 is in general thinner than the one derived from the H_2O-O_3 pair, confirming the results of Hegglin et al. (2009).

The comparison between ECHAM5/MESSy and the aircraft observations has shown that the CCM is able to reproduce the differences among the different campaigns related to the peculiar regions and seasons (see, for instance, Fig. 2 and Fig. 5), though a free running simulation without dynamical nudging has been used and observations have not been filtered to remove the impact of small scale and local processes (such as convection) on the measured mixing ratios of the target species.

Even if restricted to a single CCM and the M55 observational dataset, the analyses performed in this paper show that the use of specific diagnostics for the analysis of different datasets can highlight the average features of the TTL vertical structure and allow to roughly estimate the TTL thickness. Until now, the extratropical transition

region has been diagnosed using such tools mainly applied to satellite data, and the extratropical UT/LS depth has been derived from both the vertical tracer gradients and the tracer-tracer correlations, but few applications can be found in the literature concerning the TTL. The suite of diagnostics presented in this paper can contribute to give representativeness to geographically sparse or limited in-situ observations, and can be profitably applied to satellite data, as extensively done in the extra-tropics, and to CCM data.

References

Andrews, A. E., Boering, K. A., Daube, B. C., Wofsy, S. C., Hintsa, E. J., Weinstock, E. M., and Bui, T. P.: Empirical age spectra for the lower tropical stratosphere from in situ observations of CO_2: Implications for stratospheric transport, J. Geophys. Res., 104(D21), 26581–2659, 1999. 11661

Brewer, A. W.: Evidence for a world circulation provided by the measurements of helium and water vapour distribution in the stratosphere, Q. J. Roy. Meteorol. Soc., 75, 351–363, 1949. 11661, 11669, 11673

Brunner, D., Siegmund, P., May, P. T., Chappel, L., Schiller, C., Müller, R., Peter, T., Fueglistaler, S., MacKenzie, A. R., Fix, A., Schlager, H., Allen, G., Fjaeraa, A. M., Streibel, M., and Harris, N. R. P.: The SCOUT-O3 Darwin Aircraft Campaign: rationale and meteorology, Atmos. Chem. Phys., 9, 93–117, 2009, http://www.atmos-chem-phys.net/9/93/2009/. 11664, 11672

Cagnazzo, C., Manzini, E., Giorgetta, M. A., Forster, P. M. De F., and Morcrette, J. J.: Impact of an improved shortwave radiation scheme in the MAECHAM5 General Circulation Model, Atmos. Chem. Phys., 7, 2503–2515, 2007, http://www.atmos-chem-phys.net/7/2503/2007/. 11665

Diagnostics of the TTL

E. Palazzi et al.

◀ | ▶

◀ | ▶

Back | Close

Full Screen / Esc

Printer-friendly Version

Interactive Discussion

Chaboureau, J.-P., Cammas, J.-P., Duron, J., Mascart, P. J., Sitnikov, N. M., and Voessing, H.-J.: A numerical study of tropical cross-tropopause transport by convective overshoots, Atmos. Chem. Phys., 7, 1731–1740, 2007, http://www.atmos-chem-phys.net/7/1731/2007/. 11664, 11665

5 Corti, T., Luo, B. P., de Reus, M., Brunner, D., Cairo, F., Mahoney, M. J., Martucci, G., Matthey, R., Mitev, V., dos Santos, F. H., Schiller, C., Shur, G., Sitnikov, N. M., Spelten, N., Voessing, H. J., Borrmann, S., and Peter, T.: Unprecedented evidence for deep convection hydrating the tropical stratosphere, Geophys. Res. Lett., 35, L10810, doi:10.1029/2008GL033641, 2008. 11665, 11674

10 Folkins, I., Loewenstein, M., Podolske, J., Oltmans, S. J., and Proffitt, M.: A barrier to vertical mixing at 14 km in the tropics: Evidence from ozonesondes and aircraft measurements, J. Geophys. Res., 104(D18), 22095–22102, 1999. 11668, 11671

Fueglistaler, S., Bonazzola, M., Haynes, P., and Peter, Th.: Stratospheric water vapor predicted from the Lagrangian temperature history of air entering the stratosphere in the tropics, J.

15 Geophys. Res., 110, D08107, doi:10.1029/2004JD005516, 2005. 11661

Fueglistaler, S., Dessler, A. E., Dunkerton, T. J., Folkins, I., Fu, Q., and Mote, P. W.: Tropical tropopause layer, Rev. Geophys., 47, RG1004, doi:10.1029/2008RG000267, 2009. 11662, 11667

Gettelman, A. and Forster, P. M. de F.: A climatology of the tropical tropopause layer, J. Meteo-

20 rol. Soc. Jpn., 80, 911–924, 2002. 11668

Gettelman, A. and Birner, T.: Insights into Tropical Tropopause Layer processes using global models, J. Geophys. Res., 112, D23104, doi:10.1029/2007JD008945, 2007. 11662

Giorgetta, M. A., Manzini, E., Roeckner, E., Esch, M., and Bengtsson, L.: Climatology and Forcing of the Quasi-Biennial Oscillation in the MAECHAM5 Model, J. Climate, 19(6), 3882–

25 3901, 2006. 11665

Hegglin, M. I., Brunner, D., Peter, T., Hoor, P., Fischer, H., Staehelin, J., Krebsbach, M., Schiller, C., Parchatka, U., and Weers, U.: Measurements of NO, NO_y, N_2O, and O_3 during SPURT: implications for transport and chemistry in the lowermost stratosphere, Atmos. Chem. Phys., 6, 1331–1350, 2006,

30 http://www.atmos-chem-phys.net/6/1331/2006/. 11668

Hegglin, M. I. and Shepherd, T. G.: O_3-N_2O correlations from the Atmospheric Chemistry Experiment: Revisiting a diagnostic of transport and chemistry in the stratosphere, J. Geophys. Res., 112, D19301, doi:10.1029/2006JD008281, 2007. 11670, 11679

Hegglin, M. I., Boone, C. D., Manney, G. L., and Walker, K. A.: A global view of the extratropical tropopause transition layer from Atmospheric Chemistry Experiment Fourier Transform Spectrometer O_3, H_2O, and CO, J. Geophys. Res., 114, D00B11, doi:10.1029/2008JD009984, 2009. 11663, 11669, 11670, 11673, 11676, 11681

5 Highwood, E. J. and Hoskins, B. J.: The tropical tropopause, Q. J. Roy. Meteorol. Soc., 124(549), 1579–1604, 1998. 11668

Holton, J., Haynes, P., McIntyre, M., Douglass, A., Rood, R., and Pfister L.: Stratosphere-Troposphere Exchange, Rev. Geophys., 33(4), 403–439, 1995. 11661

Hoor, P., Gurk, C., Brunner, D., Hegglin, M. I., Wernli, H., and Fischer, H.: Seasonality and
10 extent of extratropical TST derived from in-situ CO measurements during SPURT, Atmos. Chem. Phys., 4, 1427–1442, 2004,
http://www.atmos-chem-phys.net/4/1427/2004/. 11668

Jöckel, P., Sander, R., Kerkweg, A., Tost, H., and Lelieveld, J.: Technical Note: The Modular Earth Submodel System (MESSy) – a new approach towards Earth System Modeling, At-
15 mos. Chem. Phys., 5, 433–444, 2005,
http://www.atmos-chem-phys.net/5/433/2005/. 11666

Jöckel, P., Tost, H., Pozzer, A., Brühl, C., Buchholz, J., Ganzeveld, L., Hoor, P., Kerkweg, A., Lawrence, M. G., Sander, R., Steil, B., Stiller, G., Tanarhte, M., Taraborrelli, D., van Aardenne, J., and Lelieveld, J.: The atmospheric chemistry general circulation model
20 ECHAM5/MESSy1: consistent simulation of ozone from the surface to the mesosphere, Atmos. Chem. Phys., 6, 5067–5104, 2006,
http://www.atmos-chem-phys.net/6/5067/2006/. 11665

Kerkweg, A., Sander, R., Tost, H., and Jöckel, P.: Technical note: Implementation of prescribed (OFFLEM), calculated (ONLEM), and pseudo-emissions (TNUDGE) of chemical species in
25 the Modular Earth Submodel System (MESSy), Atmos. Chem. Phys., 6, 3603–3609, 2006,
http://www.atmos-chem-phys.net/6/3603/2006/. 11666

Konopka, P., Günther, G., Müller, R., dos Santos, F. H. S., Schiller, C., Ravegnani, F., Ulanovsky, A., Schlager, H., Volk, C. M., Viciani, S., Pan, L. L., McKenna, D.-S., and Riese, M.: Contribution of mixing to upward transport across the tropical tropopause layer (TTL), Atmos. Chem.
30 Phys., 7, 3285–3308, 2007,
http://www.atmos-chem-phys.net/7/3285/2007/. 11675

Kyrö, E., Kivi, R., Turunen, T., Aulamo, H., Rudakov, V. V., Khattatov, V. V., MacKenzie, A. R., Chipperfield, M. P., Lee, A. M., Stefanutti, L., and Ravegnani, F.: Ozone measurements

Diagnostics of the TTL

E. Palazzi et al.

during the Airborne Polar Experiment: Aircraft instrument validation; isentropic trends; and hemispheric fields prior to the 1997 Arctic ozone depletion, J. Geophys. Res., 105, 14599–14611, 2000. 11688

Lelieveld, J., Brühl, C., Jöckel, P., Steil, B., Crutzen, P. J., Fischer, H., Giorgetta, M. A., Hoor, P., Lawrence, M. G., Sausen, R., and Tost, H.: Stratospheric dryness: model simulations and satellite observations, Atmos. Chem. Phys., 7, 1313–1332, 2007, http://www.atmos-chem-phys.net/7/1313/2007/. 11667, 11674

Liu, C., Zipser, E., Garrett, T., Jiang, J. H., and Su, H.: How do the water vapor and carbon monoxide tape recorders start near the tropical tropopause?, Geophys. Res. Lett., 34, L09804, doi:10.1029/2006GL029234, 2007. 11667

Lohmann, U. and Roeckner, E: Design and performance of a new cloud microphysics scheme developed for the ECHAM general circulation model, Clim. Dynam., 12(8), 557–572, 1996. 11666

Mote, P., Rosenlof, W. K., McIntyre, M., Carr, E., Gille, J., Holton, J., Kinnersley, J., Pumphrey, H., Russell III, J. M., and Waters, J.: An atmospheric tape recorder: The imprint of tropical tropopause temperatures on stratospheric water vapor, J. Geophys. Res., 101, 3989–4006, 1996. 11661

Neu, J. L., Sparling, L. C., and Plumb, R. A.: Variability of the subtropical "edges" in the stratosphere, J. Geophys. Res., 108(D15), 4482, doi:10.1029/2002JD002706, 2003. 11679

Pan, L. L., Randel, W. J., Gary, B. L., Mahoney, M. J., and Hintsa, E. J.: Definitions and sharpness of the extratropical tropopause: A trace gas perspective, J. Geophys. Res., 109, D23103, doi:10.1029/2004JD004982, 2004. 11668

Pan, L. L., Wei, J. C., Kinnison, D. E., Garcia, R. R., Wuebbles, D. J., and Brasseur, J. P: A set of diagnostics for evaluating chemistry-climate models in the extratropical tropopause region, J. Geophys. Res., 112, D09316, doi:10.1029/2006JD007792, 2007. 11662, 11663, 11668, 11669, 11676, 11680

Park, S., Jiménez, R., Daube, B. C., Pfister, L., Conway, T. J., Gottlieb, E. W., Chow, V. Y., Curran, D. J., Matross, D. M., Bright, A., Atlas, E. L., Bui, T. P., Gao, R.-S., Twohy, C. H., and Wofsy, S. C.: The CO_2 tracer clock for the Tropical Tropopause Layer, Atmos. Chem. Phys., 7, 3989–4000, 2007, http://www.atmos-chem-phys.net/7/3989/2007/. 11661

Plumb, R. A.: Tracer-tracer relationships in the stratosphere, Rev. Geophys., 45, RG4005, doi:10.1029/2005RG000179, 2007. 11669

Prinn, R. G., Weiss, R. F., Fraser, P. J., Simmonds, P. G., Cunnold, D. M., Alyea, F. N., O'Doherty, S., Salameh, P., Miller, B. R., Huang, J., Wang, R. H. J., Hartley, D. E., Harth, C., Steele, L. P., Sturrock, G., Midgley, P. M., and McCulloch, A.: A history of chemically and radiatively important gases in air deduced from ALE/GAGE/AGAGE, J. Geophys. Res., 105(D14), 17751–17792, 2000. 11675

Randel, W. J., Wu, F., Gettelman, A., Russell III, J. M., Zawodny, J. M., and Oltmans, S. J.: Seasonal variation of water vapor in the lower stratosphere observed in Halogen Occultation Experiment data, J. Geophys. Res., 106(D13), 14313–14325, 2001. 11661

Randel, W. J., Park, M., Wu, F., and Livesey, N.: A Large Annual Cycle in Ozone above the Tropical Tropopause Linked to the Brewer-Dobson Circulation, J. Atmos. Sci., 64, 4479–4488, 2007. 11669

Roeckner, E., Bäuml, G., Bonaventura, L., Brokopf, R., Esch, M., Giorgetta, M., Hagemann, S., Kirchner, I., Kornblueh, L., Manzini, E., Rhodin, A., Schlese, U., Schulzweida, U., and Tompkins, A.: The atmospheric general circulation model ECHAM5. PART I: Model description, Max Planck Institute for Meteorology, MPI-Report 349, online available at: http://www.mpimet.mpg.de/fileadmin/models/echam/mpi_report_349.pdf, 2003. 11665

Roeckner, E., Brokopf, R., Esch, M., Giorgetta, M., Hagemann, S., Kornblueh, S., Manzini, E., Schlese U., and Schulzweida, U.: Sensitivity of Simulated Climate to Horizontal and Vertical Resolution in the ECHAM5 Atmosphere Model, J. Climate, 19(16), 3771–3791, doi:10.1175/JCLI3831.1, 2006. 11665

Sherwood, S. C. and Dessler, A. E.: A model for transport across the tropical tropopause, J. Atmos. Sci., 58, 765–779, 2001. 11668

Schoeberl, M. R., Duncan, B. N., Douglass, A. R., Waters, J., Livesey, N., Read, W., and Filipiak, M.: The carbon monoxide tape recorder, Geophys. Res. Lett., 33, L12811, doi:10.1029/2006GL026178, 2006. 11661

Shuckburgh, E., Norton, W., Iwi, A., and Haynes, P.: Influence of the quasi-biennial oscillation on isentropic transport and mixing in the tropics and subtropics, J. Geophys. Res., 106(D13), 14327–14337, 2001. 11675

Sparling, L. C.: Statistical perspectives on stratospheric transport, Rev. Geophys., 38(3), 417–436, 2000. 11678, 11679

Stefanutti, L., Mackenzie, A. R., Santacesaria, V., Adriani, A., Balestri, S., Borrmann, S., Khattov, V., Mazzinghi, P., Mitev, V., Rudakov, V., Schiller, C., Toci, G., Volk, C. M., Yushkov, V., Flentje, H., Kiemle, C., Redaelli, G., Carslaw, K. S., Noon, K., and Peter, Th.: The APE-

THESEO Tropical Campaign: An Overview, J. Atmos. Chem., 48(1), 1–33, 2004. 11664

Thompson, A. M. and Witte, J. C.: SHADOZ (Southern Hemisphere Additional Ozonesondes): A new data set for the earth science community, Earth Observer, 11(4), 27–30, 1999. 11672

Thuburn, J. and Craig, G. C.: On the temperature structure of the tropical substratosphere, J. Geophys. Res., 107(D2), 4017, doi:10.1029/2001JD000448, 2002. 11668

Vaughan, G., Schiller, C., MacKenzie, A. R., Bower, K., Peter, T., Schlager, H., Harris N. R. P., and May, P. T.: SCOUT-O3/ACTIVE: High-altitude aircraft measurements around deep tropical convection, B. Am. Meteorol. Soc., 89(5), 647–662, 2008. 11664

Viciani, S., D'Amato, F., Mazzinghi, P., Castagnoli, F., Toci, G., and Werle, P. A.: Cryogenically operated laser diode spectrometer for airborne measurement of stratospheric trace gases, Appl. Phys. B, 90(3–4), 581–592, 2008. 11688

Volk, C. M., Riediger, O., Strunk, M., Schmidt, U., Ravegnani, F., Ulanovsky, A., and Rudakov, V.: In situ Tracer Measurements in the Tropical Tropopause Region During APE-THESEO, Eur. Comm. Air Pollut. Res. Report 73, 661–664, 2000. 11688

Vömel, H., Oltmans, S. J., Johnson, B. J., Hasebe, F., Shiotani, M., Fujiwara, M., Nishi, N., Agama, M., Cornejo, J., Paredes, F., and Enriquez, H.: Balloon-borne observations of water vapor and ozone in the tropical upper troposphere and lower stratosphere, J. Geophys. Res., 107(D14), 4210, doi:10.1029/2001JD000707, 2002. 11668

World Meteorological Organisation (WMO): Definition of the tropopause, WMO Bull., 6, p. 136, 1957. 11668

Yushkov V., Oulanovsky, A., Lechenuk, N., Rudakov, I., Arshinov, K., Tikhonov, F., Stefanutti, L., Ravegnani, F., Bonafe, U., and Georgiadis, T.: A chemilumineschent Analyser for stratospheric Measurements of the Ozone Concentration (FOZAN), J. Atmos. Ocean. Tech., 16, 1345–1350, 1999. 11688

Zöger, M., Afchine, A., Eicke, N., Gerhards, M.-T., Klein, E., McKenna, D. S., Mörschel, U., Schmidt, U., Tan, V., Tuitjer, F., Woyke, T., and Schiller, C.: Fast in situ stratospheric hygrometers: A new family of balloon-borne and airborne Lyman α photofragment fluorescence hygrometers, J. Geophys. Res., 104(D1), 1807–1816, doi:10.1029/1998JD100025, 1999. 11688

Title Page

Abstract | Introduction

Conclusions | References

Tables | Figures

◄ | ►

◄ | ►

Back | Close

Full Screen / Esc

Printer-friendly Version

Interactive Discussion

Table 1. List and principal characteristics of the instruments onboard the Geophysica aircraft during APE-THESEO, TROCCINOX, SCOUT-Darwin and SCOUT-AMMA campaigns. In this study, ozone data come from FOZAN instrument for all the campaigns except than APE-THESEO, for which data from ECOC instrument have been considered. CO mixing ratios were not measured during APE-THESEO.

Instrument	Measured parameter	Technique	Averaging time	Accuracy	Precision
FOZAN Yushkov et al. (1999)	O_3	Dye chemi-luminescence	1 s	0.01 ppmv	8%
ECOC Kyrö et al. (2000)	O_3	ECC	5 s	5%	2%
FISH Zöger et al. (1999)	H_2O (total)	Lyman-α photo-fragment flourescence	1 s	6%	0.2 ppmv
HAGAR Volk et al. (2000)	N_2O	GC-ECG	70 s	2%	1%
COLD Viciani et al. (2008)	CO	TDL	4s	9%	1%

Table 2. Location and time period of the four aircraft campaigns. The number of model grid points within the latitude-longitude box for each campaign is indicated.

Campaign	Time	Region	Lat-Lon (°)	QBO	Model grid points
APE-THESEO	February–March 1999	Seychelles	lat:[−20,2] lon:[45,60]	beginning of positive QBO (easterly winds)	48
TROCCINOX	January–February 2005	Brazil	lat:[−24,−14] lon:[-55,-40]	positive QBO	20
SCOUT-Darwin	November–December 2005	Australia	lat:[−24,−5] lon:[127,135]	negative QBO	21
SCOUT-AMMA	August 2006	West-Africa	lat:[−14,28] lon:[-8,4]	positive QBO	60
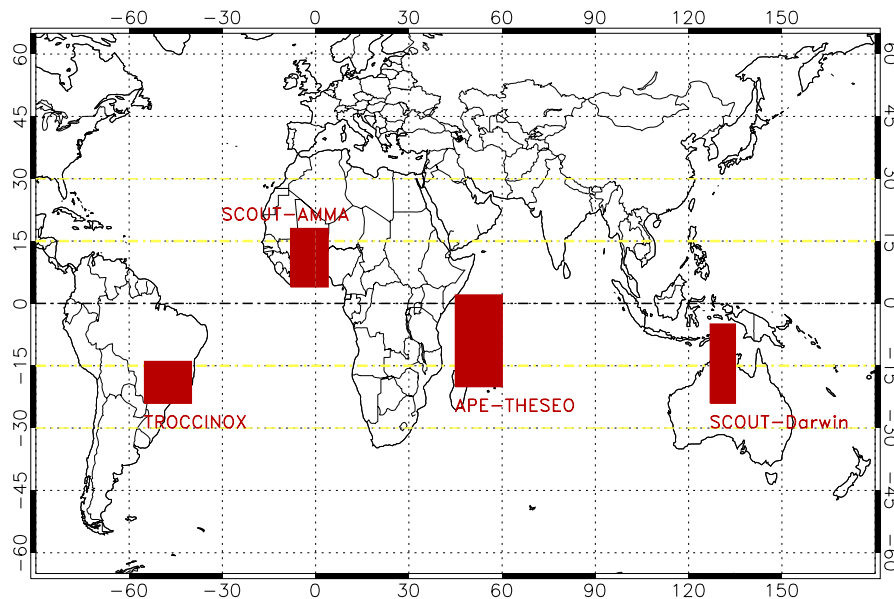
Fig. 1. Geographic location of the four measurement campaigns considered in this study. The red boxes indicate the areas where most flights were carried out (the transfer flights are not included in our analysis) and comparison between the observations and the model data has actually been performed.
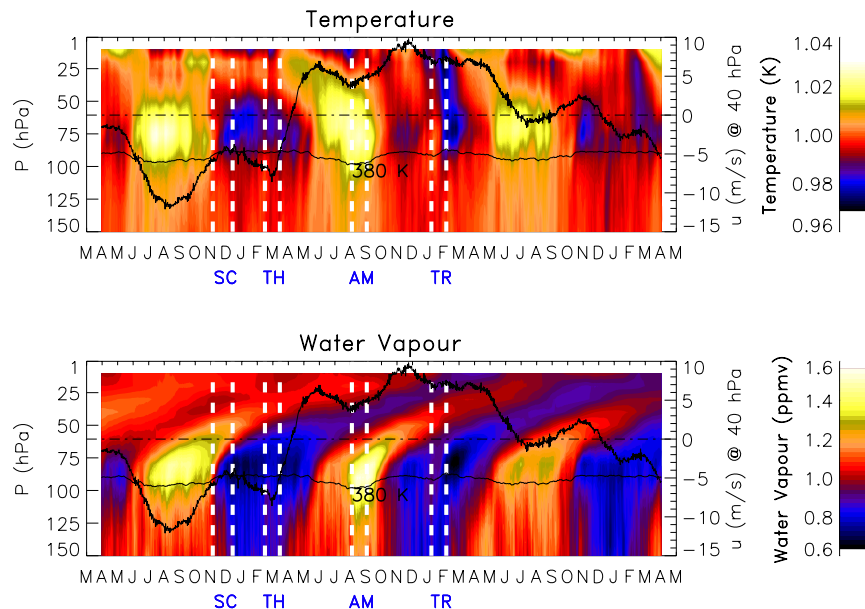
Fig. 2. Variation of 15°S and 15°N mean ECHAM5/MESSy temperature and water vapour after dividing by the mean value at each levels. Each panel also shows the isentropic surface at θ=380 K (here used as a proxy of the tropical tropopause) and the zonal mean zonal wind at 40 hPa. The dashed vertical lines mark the temporal domains of the four measurement campaigns (SC=SCOUT-Darwin, TH=APE-THESEO, AM=SCOUT-AMMA, TR=TROCCINOX) and locate them within the three model years.
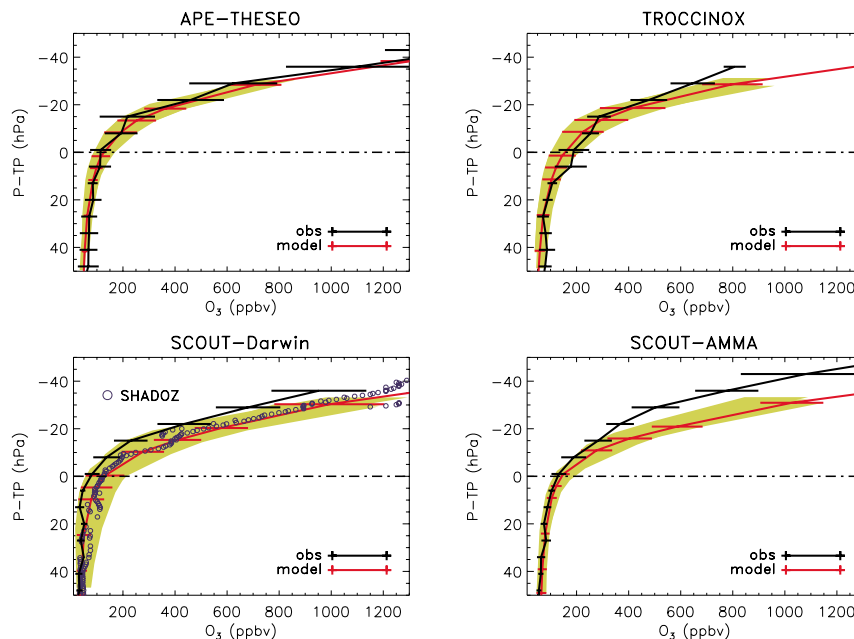
Fig. 3. Mean vertical profiles of O_3 mixing ratios with standard deviations as a function of pressure relative to the to the thermal tropopause (TP=Tropopause Pressure) for M55-Geophysica campaigns (black line) and ECHAM5/MESSy (red line). For the model we have reported the line corresponding to the year having the same QBO phase of the campaign year. The shaded area includes the three model years with their standard deviations. The black dash-dotted line indicates the thermal tropopause from temperature and pressure observations. Blue circles in the bottom left plot indicate the measurements performed over the Fiji Islands in the time period corresponding to the SCOUT-Darwin campaign by ozonosondes belonging to the SHADOZ network.
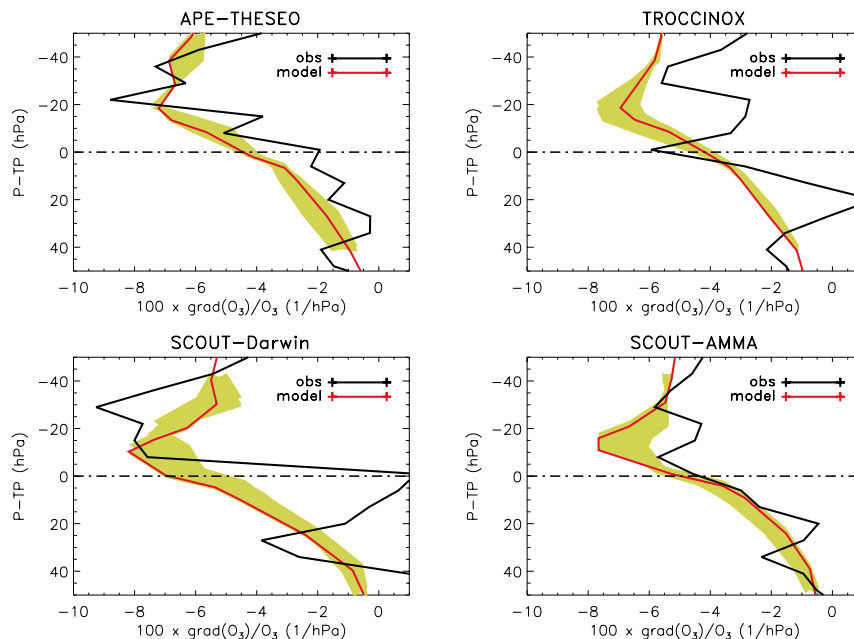
Fig. 4. Relative vertical ozone gradients (ratio between the ozone gradient and its concentration) in tropopause coordinate (TP=Tropopause Pressure) for M55-Geophysica campaigns and ECHAM5/MESSy. Color code is the same as Fig. 3. The black dash-dotted line indicates the thermal tropopause pressure level, calculated from temperature and pressure observations.
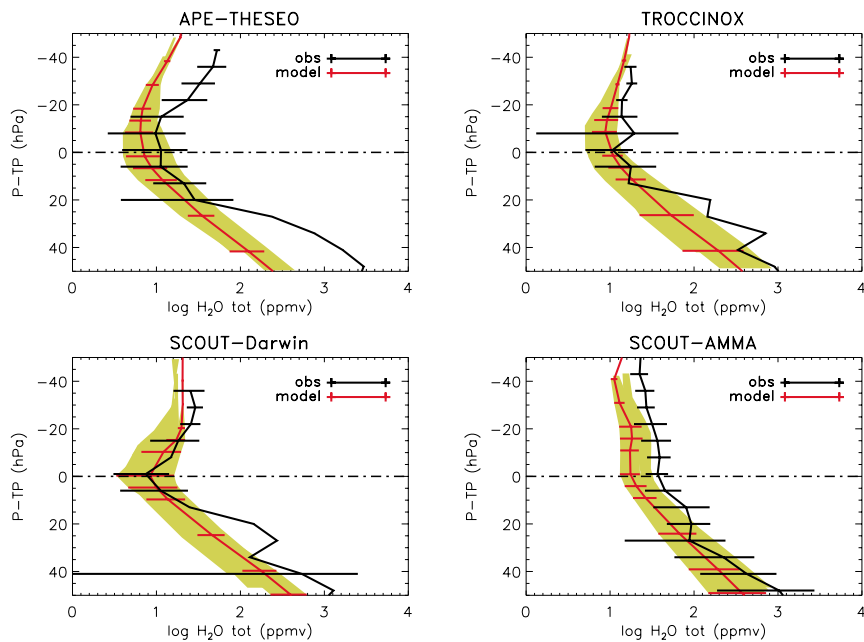
Fig. 5. The same as Fig. 3, for H_2O. A logarithmic scale has been used for H_2O mixing ratios.

Title Page

Abstract   Introduction

Conclusions   References

Tables   Figures

◄   ►

Back   Close

Full Screen / Esc

Printer-friendly Version

Interactive Discussion
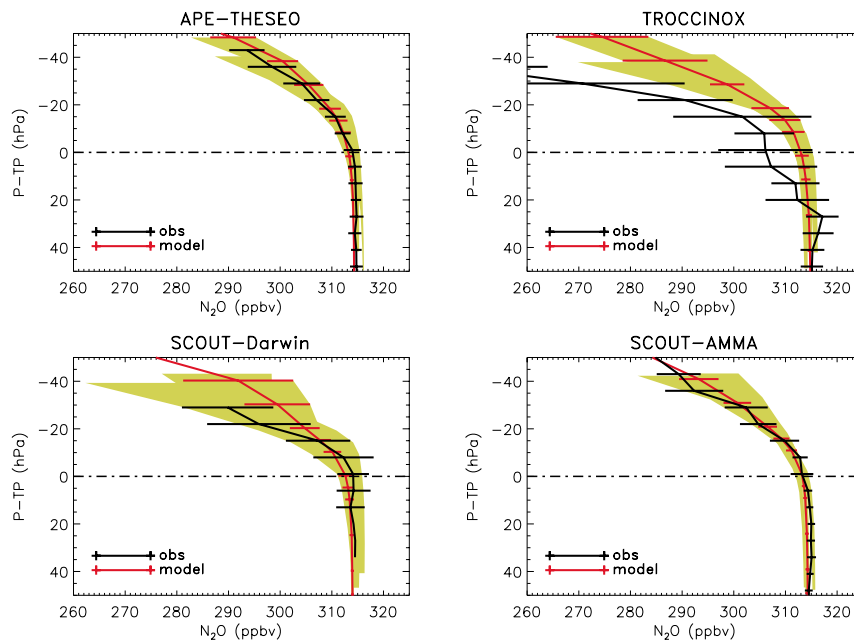
Fig. 6. The same as Fig. 3, for N_2O.
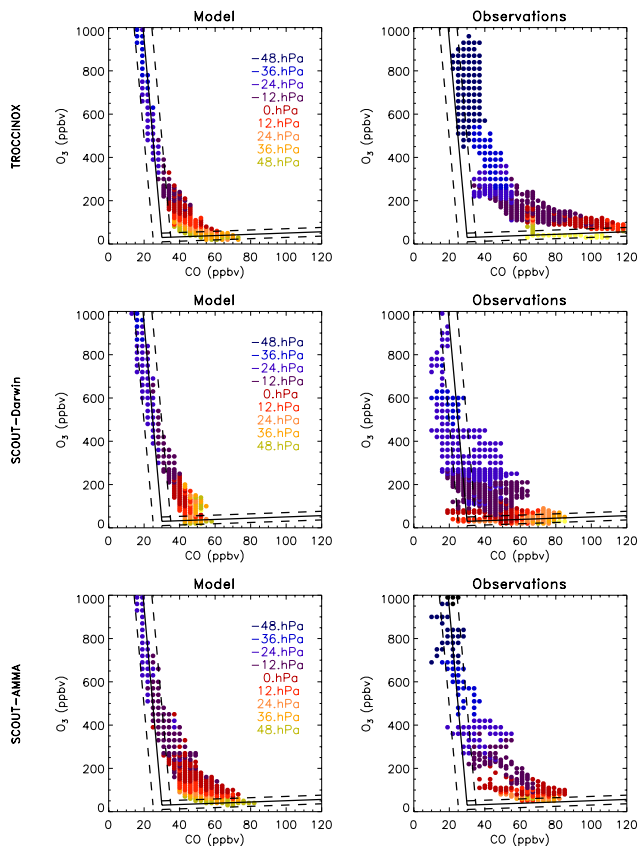
Fig. 7. CO-O_3 correlations for ECHAM5/MESSy (left column) and the observations (right column), relative to the regions and time periods of TROCCINOX, SCOUT-Darwin, and SCOUT-AMMA campaigns (from top to bottom), divided by color according to 12 hPa-thick pressure ranges whose central value is indicated in the legend. Black solid lines indicate fits (as explained in the text) to tropospheric and stratospheric branches.
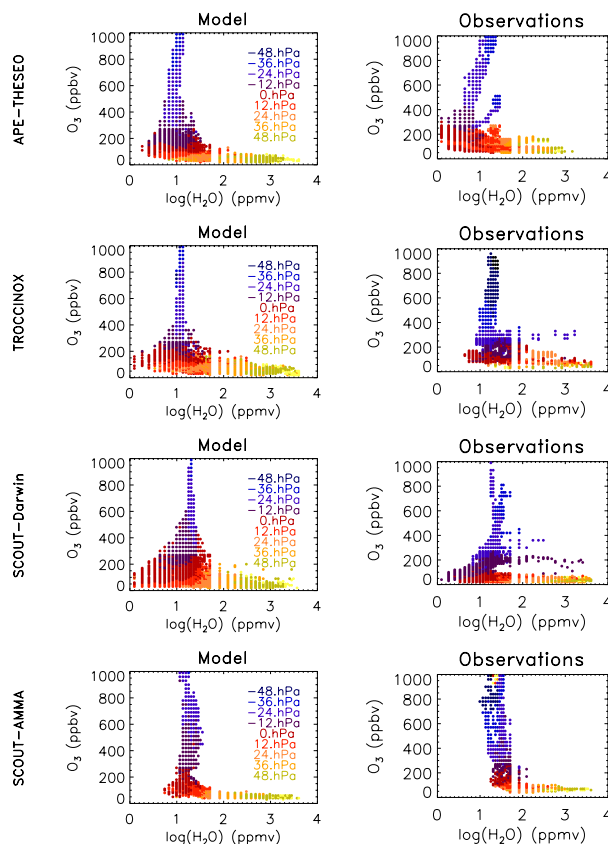
Fig. 8. H_2O-O_3 correlations for ECHAM5/MESSy (left column) and the observations (right column), relative to the regions and time periods of APE-THESEO, TROCCINOX, SCOUT-Darwin, and SCOUT-AMMA campaigns (from top to bottom), divided by color according to 12hPa-thick pressure ranges whose central value is indicated in the legend.

Fig. 9. Joint probability distribution functions (PDFs) of the H_2O-O_3 correlation for the region and time period relative to the SCOUT-Darwin campaign. Left: ECHAM5/MESSy; right: observations.